The Astrophysical Journal Letters, 952:L32 (8pp), 2023 August 1 https://doi.org/10.3847/2041-8213/ace779

Collapsar Black Holes Are Likely Born Slowly Spinning

Ore Gottlieb[1], Jonatan Jacquemin-Ide[1], Beverly Lowell[1], Alexander Tchekhovskoy[1], and Enrico Ramirez-Ruiz[2]
[1] Center for Interdisciplinary Exploration & Research in Astrophysics (CIERA), Physics & Astronomy, Northwestern University, Evanston, IL 60202, USA; ore@northwestern.edu
[2] Department of Astronomy and Astrophysics, University of California, Santa Cruz, CA 95064, USA
Received 2023 February 15; revised 2023 May 12; accepted 2023 May 17; published 2023 July 31

Abstract

Collapsing stars constitute the main black hole (BH) formation channel, and are occasionally associated with the launch of relativistic jets that power γ-ray bursts (GRBs). Thus, collapsars offer an opportunity to infer the natal (before spin-up/down by accretion) BH spin directly from observations. We show that once the BH saturates with a large-scale magnetic flux, the jet power is dictated by the BH spin and mass accretion rate. Core-collapse simulations by Halevi et al. and GRB observations favor stellar density profiles that yield an accretion rate of $\dot{m} \approx 10^{-2}\,M_{\odot}\ \mathrm{s}^{-1}$, weakly dependent on time. This leaves the spin as the main factor that governs the jet power. By comparing the jet power to characteristic GRB luminosities, we find that the majority of BHs associated with jets are likely born slowly spinning with a dimensionless spin of $a \simeq 0.2$, or $a \simeq 0.5$ for wobbling jets, with the main uncertainty originating in the unknown γ-ray radiative efficiency. This result could be applied to the entire core-collapse BH population, unless an anticorrelation between the stellar magnetic field and angular momentum is present. In a companion paper, Jacquemin-Ide et al., we show that regardless of the natal spin, the extraction of BH rotational energy leads to spin-down to $a \lesssim 0.2$, consistent with gravitational-wave observations. We verify our results by performing the first 3D general-relativistic magnetohydrodynamic simulations of collapsar jets with characteristic GRB energies, powered by slowly spinning BHs. We find that jets of typical GRB power struggle to escape from the star, providing the first numerical indication that many jets fail to generate a GRB.

Unified Astronomy Thesaurus concepts: Stellar mass black holes (1611); Black hole physics (159); Astrophysical black holes (98); Gamma-ray bursts (629); Core-collapse supernovae (304); Magnetohydrodynamical simulations (1966)

1. Introduction

When the core of a massive star exhausts its nuclear fuel, it collapses under its own gravity to form a protoneutron star (PNS). If the PNS accretes mass above $M_{\rm NS,max} \gtrsim 2.2\,M_{\odot}$ (Margalit & Metzger 2017; Aloy & Obergaulinger 2021; Obergaulinger & Aloy 2022), then it undergoes a further collapse to form a black hole (BH). As a nonnegligible fraction of all core-collapse supernovae ultimately produce a BH (e.g., Kochanek 2015), collapsing stars constitute the main BH formation channel in the Universe. The BH initially interacts with the dense stellar envelope, gaining mass and angular momentum. At these early times, the BH vicinity is opaque to electromagnetic (EM) radiation, so the BH early evolution is observationally out of reach.

Long after the BH formed and the progenitor star is gone, the BH may become involved in new astrophysical processes, such as accretion or merger, that trigger EM emission from which we can infer the BH properties, e.g., mass and spin (see Middleton 2016; Reynolds 2021 for reviews). In addition to EM signals, the first gravitational-wave detections of binary BH mergers by LIGO/Virgo/KAGRA (LVK) also provide clues regarding the BH nature. For example, different studies have consistently found that premerger BHs spin slowly (Farr et al. 2017; Tiwari et al. 2018; Roulet & Zaldarriaga 2019; Abbott et al. 2020; Hoy et al. 2022; but see also Safarzadeh et al. 2020). However, as we show in a companion paper, the inferred low spin might be an indication of a substantial BH spin-down rather than a low natal spin—the spin with which the BH forms (Jacquemin-Ide et al. 2023). Thus, while EM and gravitational-wave detections can shed light on the resultant BH properties after mass accretion, and spin-down/up, the natal BH properties are challenging to study observationally. It thus remains unclear whether BHs are born slowly spinning or are spun down after their formation.

The natal BH spin can be estimated on theoretical grounds. Fuller & Ma (2019) and Belczynski et al. (2020) found efficient angular momentum transport in stars via the magnetic Tayler instability, such that newly born BHs in massive stars maintain a low dimensionless spin $a \approx 10^{-2}$, where a varies from $a = 0$ (nonspinning BH) to $a = 1$ (maximally spinning BH). This result is consistent with the natal BH spin that follows the collapse of a millisecond PNS

$$a \simeq 0.03\left(\frac{R_{\rm NS}}{10\ \mathrm{km}}\right)^2 \frac{1\mathrm{ms}}{P}\frac{3\,M_{\odot}}{M_{\rm NS,max}}, \quad (1)$$

where $R_{\rm NS}$ is the PNS radius and P is the PNS spin period. We stress that both of those quantities could be significantly different than the canonical values in Equation (1), depending on the equation of state, stellar angular momentum, etc. In such cases, the PNS may give birth to a rapidly spinning BH (e.g., Aloy & Obergaulinger 2021; Obergaulinger & Aloy 2022). Additionally, there is a growing evidence that the majority of the BHs' very massive progenitors belong to multistar systems (Kobulnicky & Fryer 2007; Smith et al. 2011; Sana et al. 2012; Duchêne & Kraus 2013; Offner et al. 2014). The companion star may spin up the BH progenitor star, and consequently the

newly born BH itself. However, stellar population simulations show that the rotational velocity of the progenitor external shells is just a few hundred kilometers per second (de Mink et al. 2013). For a strong coupling between the stellar core and envelope, as suggested by Fuller & Ma (2019), BHs in binary stars would also form with $a \ll 1$ (Tchekhovskoy & Giannios 2015).

Massive stars in binary systems are considered to be the progenitors of long γ-ray bursts (GRBs; De Donder & Vanbeveren 1998; Fryer et al. 2007; Yoon et al. 2010), as those can supply enough angular momentum to the star to form the accretion disk required for launching relativistic jets (e.g., Izzard et al. 2004; Fryer & Heger 2005; Petrovic et al. 2005; Lee & Ramirez-Ruiz 2006; Woosley & Heger 2006; Cantiello et al. 2007). The relativistic jets that generate the GRB are considered to be electromagnetically driven (e.g., Lyutikov & Blandford 2003; Kawanaka et al. 2013), extracting rotational energy from the BH (Penrose & Floyd 1971; Blandford & Znajek 1977, hereafter BZ). Therefore, GRB jets can carry the information from the BH and provide a direct connection between the BH spin and the observed GRB power. This enables us to overcome the above uncertainties in stellar evolution models, and constrain the natal BH properties from observations, through their imprinted properties on the expelled outflows.

In this letter, we constrain the natal BH spin from observations for the first time. Many previous studies have focused on rapidly spinning BHs as the central engines powering relativistic GRB jets (Komissarov & Barkov 2009; Janiuk & Yuan 2010; Tchekhovskoy et al. 2011; Aloy & Obergaulinger 2021; Gottlieb et al. 2022a, 2022b; Bavera et al. 2022; Fujibayashi et al. 2022). Here, we argue analytically (Section 2) and numerically (Section 3) that GRB observables suggest that the majority of BHs form with a low spin. This makes low BH spins more attractive for GRB jet launching than previously thought. We verify our conclusions by presenting the first 3D general-relativistic magnetohydrodynamic (GRMHD) simulations of collapsar jets from slowly spinning BHs. We discuss the implications for jets and their progenitor stars in Section 4.

2. Why Are Jet-associated BHs Slowly Spinning?

Gottlieb et al. (2022a) performed the first 3D GRMHD simulations of collapsars that follow BZ-powered relativistic jets from the BH to outside of the star. They fixed the BH dimensionless spin to $a = 0.8$, and explored the effect of the magnetic field strength on relativistic jet launching. The simulations showed that if the magnetic field amplitude is below a certain threshold, which depends on the stellar core density, then the jets fail to launch. Interestingly, Gottlieb et al. (2022a, 2022b) found that even when the magnetic field is set at the minimum threshold for jet launching, the emerging jet is orders of magnitudes more powerful than the observed characteristic GRB luminosity.[3] This begs the question of what prelaunching conditions are required for powering typical GRBs.

[3] If the inner stellar mass density profile is roughly flat, $\rho \propto r^0$, the density needs to be low in order to result in a typical stellar mass, $\sim 20\ M_\odot$: this would result in a jet of typical GRB energy. However, such a density profile introduces two problems: (i) the jet power shows significant time evolution that is in tension with observations, and (ii) the jet engine life time that is shorter than that of observed long GRBs (Gottlieb et al. 2022a).

Gottlieb et al. (2022a) interpreted the above results with formulating a jet launching criterion that requires the BZ power, which scales quadratically with the BH spin and the magnetic flux threading the BH, to overcome the accretion power of the infalling gas. However, since they did not consider different BH spins, their jet launching and power were solely dictated by the initial magnetic field strength and accretion rate, so they could not have distinguished between the role of the magnetic field and the BH spin. Komissarov & Barkov (2009) proposed that jets are launched successfully so long as their Alfvén velocity is higher than the freefall velocity of the inflowing gas. This is to allow the MHD waves to escape from the BH ergosphere and constitute the emerging jet. According to this criterion, it is a strong enough magnetic flux, rather than a high enough BZ power, that enables a BH to launch jets against the onslaught of the infalling stellar envelope.[4] Furthermore, jet launching is numerically found to be sustained once the disk becomes magnetically arrested (MAD), which in turn takes place when the dimensionless magnetic flux (normalized by the mass accretion rate) reaches a certain threshold, $\phi_{\rm H} \approx 50$ (e.g., Tchekhovskoy 2015). In conclusion, the jet launching criterion depends solely on the magnetic flux, and is independent of the BH spin. In contrast, the jet power solely depends on the BH spin and mass accretion rate, while the magnetic flux is saturated at the MAD value and thus has no freedom to control the jet power. Our numerical simulations support these conclusions (Section 3).

Given the need for a sufficiently strong magnetic field to launch GRB jets inside a collapsing star, one way of achieving the desired (lower) characteristic power of GRB jets is by considering a lower BH dimensionless spin. The EM jet luminosity

$$L_j = \eta(a)\dot{m}c^2, \tag{2}$$

is defined as the EM energy flux leaving the BH, where $\dot{m}$ is the mass accretion rate onto the BH. The jet launching efficiency solely depends on the dimensionless BH spin (Lowell et al. 2023)

$$\eta(a) = 1.063a^4 + 0.395a^2. \tag{3}$$

Equations (2) and (3) demonstrate that if a jet is launched in an MAD state (in which the BH magnetic flux is saturated at the maximum, MAD, value), then its luminosity is governed only by the accretion rate and the BH spin.

The accretion rate is determined by the mass density profile of the stellar envelope. Recently, Halevi et al. (2023) examined the stellar density profile evolution during the PNS stage, between the onset of the core collapse and the formation of the BH. They found that all stellar evolution models, which feature steep density profiles with a power-law index of $\alpha = 2.5$ at the onset of the collapse, consistently converge to a shallower density profile with $\alpha = 1.5$ at the BH formation time. In a freefall collapse, a power-law density profile leads to mass accretion rate (Gottlieb et al. 2022a)

$$\dot{m}(\alpha) \sim t^{1-2\alpha/3}. \tag{4}$$

[4] Komissarov & Barkov (2009) found a weak dependency of the jet launching on the BH spin, denoted as κ in their work. As κ was found to change by up to a factor of 2 with the BH spin, its variance is negligible compared to the change by an order of magnitude of the magnetic field threading the BH.

Namely, $\dot{m}(\alpha = 1.5) \sim$ const. For a roughly constant jet launching efficiency, as expected in a saturated MAD state (e.g., Tchekhovskoy & Giannios 2015, and Section 3), the jet power remains constant as well, as implied by GRB observations (McBreen et al. 2002).

If indeed $\alpha = 1.5$ at the onset of the BH formation is a universal value, one can derive a universal accretion rate. All mass density profiles obtained by Halevi et al. (2023) roughly coincide with the initial profile used in the simulations performed by Gottlieb et al. (2022b). In these models, Gottlieb et al. (2022b) used a representative total stellar mass (including the BH mass) of 18.2 $M_\odot$. Their numerical results featured a roughly constant accretion rate of $\dot{m} \approx 5 \times 10^{-3}\, M_\odot\ \mathrm{s}^{-1}$, but with a moderate decrease owing to the suppression of accretion from the outflows. This accretion rate might increase linearly with the stellar mass, which may be larger by a factor of a few.[5] Thus, for a canonical accretion rate of $\dot{m} \approx 10^{-2}\, M_\odot\ \mathrm{s}^{-1}$ (as was also found in core-collapse simulations; e.g., Obergaulinger & Aloy 2022), Equations (2) and (3) dictate that the jet luminosity depends on the BH spin

$$L_j \approx 2 \times 10^{52}(1.063a^4 + 0.395a^2)\left(\frac{\dot{m}}{10^{-2}\ M_\odot\ \mathrm{s}^{-1}}\right)\ \mathrm{erg\ s}^{-1}. \tag{5}$$

For a characteristic observed isotropic equivalent γ-ray luminosity of $L_{\gamma,\mathrm{iso}} \simeq 3 \times 10^{52}\,\mathrm{erg\ s}^{-1}$ (Wanderman & Piran 2010), and opening angle $\theta_j \simeq 0.1$ (Goldstein et al. 2016), the intrinsic two-jet γ-ray luminosity is $L_\gamma \equiv L_{\gamma,\mathrm{iso}}[1 - \cos(\theta_j)] \simeq 1.5 \times 10^{50}\ \mathrm{erg\ s}^{-1}$. The jet power is determined by the poorly constrained γ-ray radiative efficiency ϵ_γ (Eichler & Waxman 2005), whose wide range from $\epsilon_\gamma \ll 1$ (Frail et al. 2001) to $\epsilon_\gamma \approx 0.8$ (e.g., Panaitescu & Kumar 2002) introduces a significant uncertainty. We choose a fiducial value of $\epsilon_\gamma = 0.5$, so the total jet luminosity is $L_j = L_\gamma/\epsilon \simeq 3 \times 10^{50}(0.5/\epsilon_\gamma)(\theta_j/0.1)^2\ \mathrm{erg\ s}^{-1}$. Plugging in Equation (5), the corresponding BH dimensionless spin is

$$a \simeq 0.18\left(\frac{0.5}{\epsilon_\gamma}\right)^{0.5}\left(\frac{\theta_j}{0.1}\right), \tag{6}$$

where the dependency on ϵ_γ, θ_j, assumes $\eta \sim a^2$, which is valid at low spins, and is a rough estimate to within a factor of a few at high spins.

In addition to the radiative efficiency, another difficulty in the above analysis is the nontrivial conversion of isotropic equivalent energy to total jet energy. Gottlieb et al. (2022b) showed that jets inevitably exhibit a wobbling motion, as we also find in all of our numerical models (Section 3). The jet wobbling is caused by the spontaneous tilt of the disk, induced by the stochastic torques applied to the disk by infalling gas. Consequently, a given observer will only see a fraction of the jet energy, so that the observed jet energy is in fact an order of magnitude lower than the true jet energy (Gottlieb et al. 2023). In such cases, the total GRB jet energy is $L_j \simeq 3 \times 10^{51}(0.5/\epsilon_\gamma)(\theta_w/0.3)^2\ \mathrm{erg\ s}^{-1}$, where θ_w is the wobble amplitude. Equation (5) dictates that in this case $a \simeq 0.48$. Lowell et al. (2023) argued that a cooled disk would have a milder equilibrium spin, $a = 0.3$, compared to a noncooled disk in which the equilibrium spin is $a = 0.1$. Thus, the jet wobbling motion might probe the cooling state of collapsar accretion disks.

[5] The accretion rate also increases with the BH mass, $\dot{m} \sim v_{\mathrm{ff}} \sim M^{1-\alpha/3}$, where v_{ff} is the freefall velocity, and thus $\dot{m} \sim M^{0.5}$ for $\alpha = 1.5$. For $\dot{m} \approx 10^{-2}\, M_\odot\ \mathrm{s}^{-1}$, the BH mass may double its mass during the jet launching, corresponding to a small nonlinear correction to the mass accretion rate.

3. Numerical Simulations

We investigate the emergence of GRB jets from slowly spinning BHs by performing the first collapsar simulations with a low BH spin, from jet launching to breakout. We build on the collapsar simulations that were recently carried out by Gottlieb et al. (2022b) using the code H-AMR (Liska et al. 2022). The main difference between the initial physical setup of the models is the lower BH spin compared to Gottlieb et al. (2022b) who set it to be $a = 0.8$. The full setups are given below. We also conduct one simulation with an anisotropic mass distribution of the stellar envelope to study the effect of a low-density polar region on the ability of weaker jets to break out from the star. Such an anisotropic density distribution can emerge, e.g., if the polar axis is vacated by rapid rotation of the envelope (e.g., Fujibayashi et al. 2020). However, stellar population simulations show that the stellar angular density profile is homogeneous to within a few percent, disfavoring a significant anisotropy (de Mink et al. 2013). Nevertheless, the anisotropy may emerge in the postcollapse stage due to neutrino–antineutrino annihilation (Eichler et al. 1989; MacFadyen & Woosley 1999; Popham et al. 1999), magnetic outflows, or PNS-powered precursor jets (e.g., Burrows et al. 2007). Those scenarios may form a low-density funnel that mitigates the relativistic jet propagation through the envelope. The remaining initial conditions are identical between all simulations, and are summarized below.

3.1. Setup

We initialize the simulations with a central BH mass of $M = 4.2\ M_\odot$ embedded in a stellar envelope of mass $M_\star = 14\, M_\odot$ and radius $R_\star = 4 \times 10^{10}$ cm. The magnetic vector potential in the star has only an azimuthal component that scales as $A_{\hat{\phi}}(r, \theta) \sim \sin(\theta)/r$, and drops to zero at the stellar surface. For code stability purposes, we set a maximum jet magnetization $\sigma = 150$, which is also the jet magnetization upon launching σ_0, or the jet asymptotic Lorentz factor. The stellar envelope undergoes solid body rotation well below the centrifugal value throughout the star, with the specific angular momentum given by[6]

$$l(r, \theta) = \begin{cases} \omega_0 r^2 \sin^2\theta & \text{for } r \leqslant 70 r_g, \\ \omega_0 (70 r_g)^2 \sin^2\theta & \text{for } r > 70 r_g, \end{cases} \tag{7}$$

where $r_g \equiv GM/c^2 = 6.3 \times 10^5$ cm is the BH gravitational radius and $\omega_0 = 50\ \mathrm{s}^{-1}$. We note that prior to the BH formation, Halevi et al. (2023) found that the innermost ($\approx 10^{8.5}$ cm) stellar shells accelerate to high velocities. Since our simulations do not have self-gravity, we set the radial velocity to zero. However, those shells will accelerate as they freefall and reach similar velocities. Importantly, the freefall time of those shells is $\lesssim$0.1 s, implying that after that time the progenitor structure is consistent with that of Halevi et al. (2023). We have verified via a direct simulation that an

[6] Note that this expression is a typo correction to the one in Gottlieb et al. (2022a, 2022d).

Table 1
The Parameters of the Different Models

Model	a	δ	t_b (s)	t_s (s)	$M_{\rm ej}/M_\star(9.2$ s)	$M_{\rm ej}/M_\star(t_s)$
$a8\delta0$	0.8	0	2.1	9.2	65%	
$a2\delta0$	0.2	0	11.5	15.5	52%	75%
$a1\delta0$	0.1	0	16	22	32%	79%
$a1\delta1$	0.1	1	3.5	9.2	21%	

Note. a is the BH dimensionless spin, δ is the mass distribution anisotropic component power-law index, t_b is the shock breakout time from the star, t_s is the simulation duration, and $M_{\rm ej}/M_\star$ is the fraction of the stellar envelope that is unbound (hydrodynamically and magnetically).

identical setup with the initial radial velocity set to the freefall velocity converges to the same mass accretion rate after a short initial transient of $t \lesssim 0.1$ s.

We explore both isotropic and anisotropic mass density profiles, with the degree of anisotropy controlled by δ

$$\rho(r,\theta) = \rho_0 \left(\frac{r}{R_\star}\right)^{-1.5} \left(1 - \frac{r}{R_\star}\right)^3 \sin^\delta(\theta), \quad (8)$$

where ρ_0 is set by $M_\star$, and depends on the value of δ. We compare our simulations with the simulation of a rapidly spinning BH and $\sigma_0 = 200$ from Gottlieb et al. (2022b). The parameters of the models are listed in Table 1.

The numerical integration is performed on a spherical grid using an ideal gas law equation of state with index of $4/3$. The radial grid is logarithmic from $0.9r_g$ to $10^6 r_g$. The number of cells in the base grid is $384 \times 96 \times 192$ in the radial, polar, and azimuthal directions, respectively. We use a local adaptive time step and three levels of adaptive mesh refinement, tuned to provide approximately the same transverse resolution across the jets at all distances (Gottlieb et al. 2022b). Thus, the maximum effective resolution of the grid is $3072 \times 768 \times 1536$. We tilt the initial conditions and the metric by 90° to avoid numerical artifacts on the jet axis, which could emerge due to the discontinuity on the polar axis (Gottlieb et al. 2022a).

3.2. Accretion and Launching

Figure 1 depicts the time evolution of the BH accretion and jet launching quantities in the different models. Figure 1(a) features comparable accretion rates in all models, with a moderate decrease in $\dot{m}$ over time, compared to the constant accretion rate expected from Equation (4). The discrepancy originates in the suppression of the mass accretion rate by the laterally extended structure of the shocked material around the jet. The weak dependency of the lateral structure on the jet power explains the comparable accretion rates between the different models. However, in the presence of a low-density region on the polar axis (model $a1\delta1$), the jet propagates fast without spilling most of its energy to the jet backflows, so its effect on the mass accretion rate diminishes. In particular, model $a1\delta1$ features $\dot{m} \propto t^{-1/4}$, whereas the other models exhibit $\dot{m} \propto t^{-3/4}$.

Figure 1(b) shows that the jet EM efficiency is dictated by the BH spin, and is consistent with Equation (3). The rapidly spinning BH (blue line) reaches an efficiency of $\eta \simeq 0.5$, whereas slowly spinning BHs exhibit $\eta \approx 10^{-2}$. All models reach those efficiencies early on, within 0.3 s after the BH

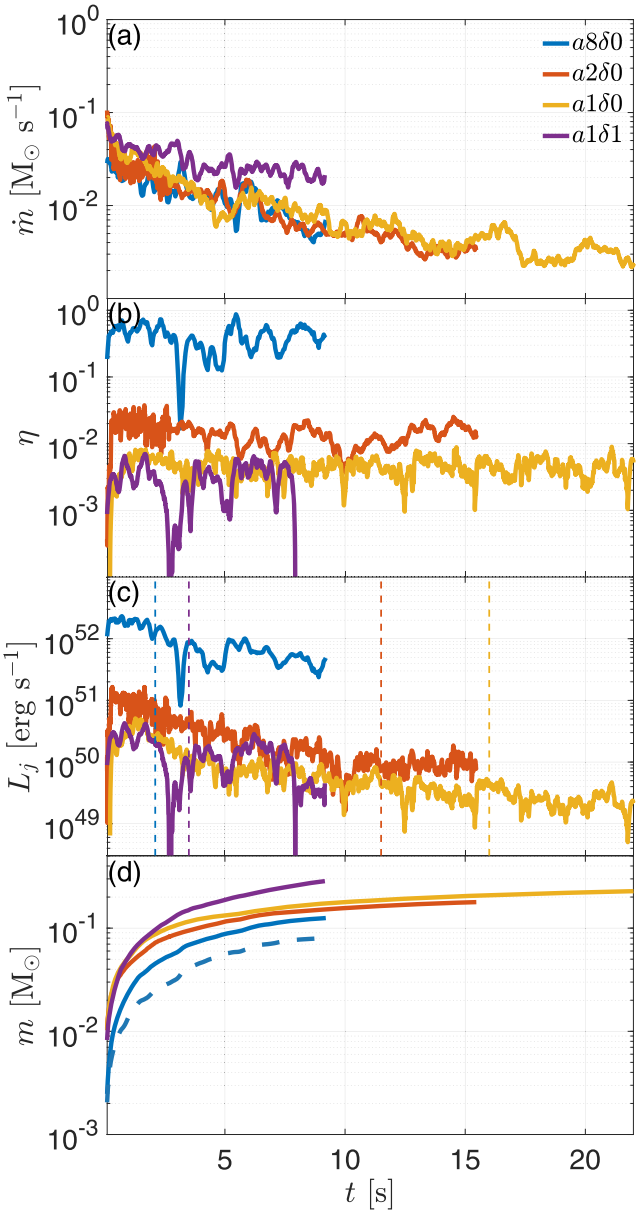

Figure 1. Smoothed time evolution of the numerical models, as measured at $3r_g$. (a) The mass accretion rate onto the BH drops moderately over time, owing to suppression by the jet structure. (b) The jet launching efficiency is in a good agreement with Lowell et al. (2023), featuring $\eta \simeq 0.5$, 0.02, and 0.005 for $a = 0.8$, 0.2, and 0.1, respectively. (c) Given the similar $\dot{m}$ in all models, BHs with $a = 0.1$ power jets that are two orders of magnitude less luminous than jets from BHs with $a = 0.8$, having $L_j \approx 10^{50}$ erg s^{-1} that is comparable with the characteristic GRB luminosity. The vertical dashed lines represent the breakout time of the outflow from the star, after which the luminosity can be observed. (d) Accreted mass. The differences in the mass accretion rate (solid lines) lead to less total accreted mass onto the BH when the jet launching and propagation are more efficient. The high efficiency $\eta \simeq 0.5$ when $a = 0.8$ indicates that half of the accreted mass is expelled as outflows, resulting in BH mass gain that is only half of the total accreted mass (dashed line).

formation, and remain quasi steady. The jet power, as shown in Figure 1(c), is the product of the mass accretion rate and launching efficiency, and thus it is also solely governed by the BH spin. While rapidly rotating BHs ($a = 0.8$) produce jets with $L_j \approx 10^{52}$ erg s^{-1} that are on the high end of the GRB energy distribution, slower ones with $a = 0.2$ give rise to jets with a typical GRB luminosity, $L_j \approx 10^{50}$ erg s^{-1}. This is the first time that a slowly spinning BH is shown to be able to

launch a relativistic jet with such power into a collapsing stellar envelope. This result is consistent with the jet launching criterion that depends only on the magnetic field threading the BH, and with the prediction that a BH with $a \approx 0.1$ launches a jet with a typical GRB energy. Due to the time evolution in the mass accretion rate, the jet luminosity also exhibits mild time evolution. Such mild evolution might be still consistent with observations since the jet is only observed after it breaks out from the star, between $\sim$10 s and a few dozen seconds, namely the observed jet evolves over less than an order of magnitude in time, thus by merely a factor of a few in luminosity. Nonetheless, obtaining constant mass accretion and jet luminosity is possible with milder density profiles of $\alpha = 1$ (Gottlieb et al. 2022a), which are also roughly consistent with the models of Halevi et al. (2023).

The roughly constant accretion rate leads to a linear growth in the accumulated accreted mass on the BH (Figure 1(d)). In model $a1\delta1$, where the accreted mass is the highest (and the unbound mass is the lowest, see Table 1), the extrapolation of the observed linear growth suggests that the BH mass doubles after $\approx$100 s. In model $a8\delta0$, the efficiency of $\eta \approx 0.5$ implies that about half of the accreted mass energy is converted to jet power, so that the BH gains only half of the accreted mass (dashed line). The lower accreted mass in model $a8\delta0$ results in a milder BH mass gain after its formation. This constitutes another argument against rapidly spinning BHs—the observed mass gap between NSs and BHs (e.g., Özel et al. 2010; Farr et al. 2011) indicates that after BHs form, they continue to accrete mass that is at least comparable to their natal mass during the stellar collapse (Belczynski et al. 2012). In order to self-consistently assess the long-term effects of initially rapidly spinning BHs, one needs to consider the BH spin-down, which we address in a companion paper (Jacquemin-Ide et al. 2023).

3.3. Jet Propagation

We find that slowly spinning collapsar BHs power jets with $L_j \approx 10^{50}\,\mathrm{erg\,s^{-1}}$, which are favored by GRB observations. While hydrodynamic and weakly magnetized jets of that power were previously shown to successfully break out from stellar envelopes (López-Cámara et al. 2013; Ito et al. 2015; López-Cámara et al. 2016; Harrison et al. 2018; Gottlieb et al. 2019; Ito et al. 2019; Gottlieb et al. 2020a, 2021b), no first-principles numerical models exist for Poynting-flux-dominated collapsar jets of that power. Here we find, for the first time, that when a jet with a typical GRB energy is launched into a spherical envelope (model $a1\delta0$), it breaks apart and invests almost all its energy in the expansion of a subrelativistic ($v \approx 0.1c$) shocked stellar material (see Figure 2). As the spherical shock breaks out, it might power a low-luminosity GRB or mildly relativistic transients such as fast blue optical transients (Gottlieb et al. 2022d). A detailed calculation of its EM signature will be conducted in future work.

The disintegration of the jet might be attributed to its initial high magnetization, which in low-power jets, gives rise to kink instabilities. However, the weak dependency of the jet kink instability criterion on the jet luminosity to density ratio, $\sim(L/\rho)^{1/6}$, and the uncertainty of the stability critical value (Bromberg & Tchekhovskoy 2016), make it difficult to determine whether the kink instability is responsible for the jet dissipation. An alternative explanation for the jet's difficulty to pierce through the stellar envelope efficiently is its intermittency along the axis of propagation, which in lower-power jets may lead to strong baryon contamination that destroys the jet (Gottlieb et al. 2020b, 2021a). The intermittent jet structure emerges due to the abrupt nature of the central engine, and the jet wobbling motion, caused by the tilt of the disk (Gottlieb et al. 2022b), which launches the jet in different directions. In other words, the effective jet head cross section becomes too large, and considering the lower jet power, its luminosity density is too low to enable an efficient jet propagation through the star.

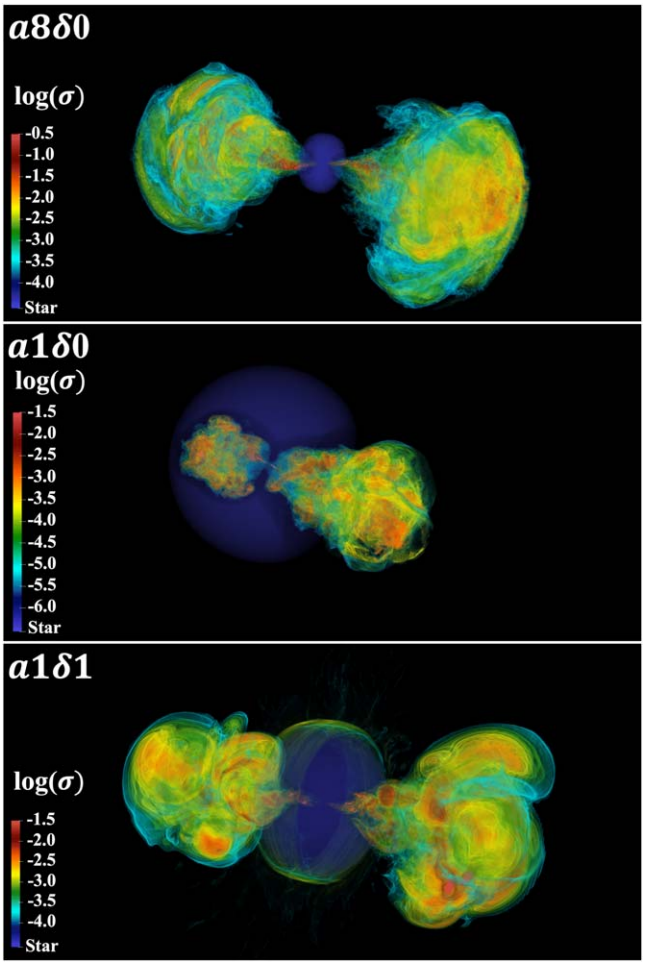

Figure 2. 3D rendering of the jet magnetization after breakout in models $a8\delta0$ (top), $a1\delta0$ (middle), and $a1\delta1$ (bottom) at $t = t_s$. While all jets find their way out from the star (dark blue), in model $a8\delta0$ the jet retains a mild magnetization and features a stratified structure, whereas in models $a1\delta0$ and $a1\delta1$ the jets fail to remain intact as they lose most of their energy to mixing with the star.

Regardless of the physical mechanism responsible for the jet destruction, a lower mass density along the rotational axis of the star may mitigate the jet propagation. In our anisotropic model with $\delta = 1$, the polar ($\theta \lesssim \theta_j$) isotropic equivalent mass is about 15 times lower than the isotropic case, equivalent to increasing the jet power by the same factor. Our simulation with $\delta = 1$ exhibits jets that quickly break out from the star, with an average head velocity inside the star of $0.4c$. Although the jet in an anisotropic star quickly breaches the envelope, its breakout characteristics are similar to those observed for jets in models $a1\delta0$ and $a2\delta0$, and are inconsistent with those inferred from GRB observables. Figure 2 portrays 3D renderings of the outflow magnetization in models $a8\delta0$ (top), $a1\delta0$ (middle), and $a1\delta1$ (bottom) after breaking out from the star (dark blue). In the first case, the powerful jet remains collimated and

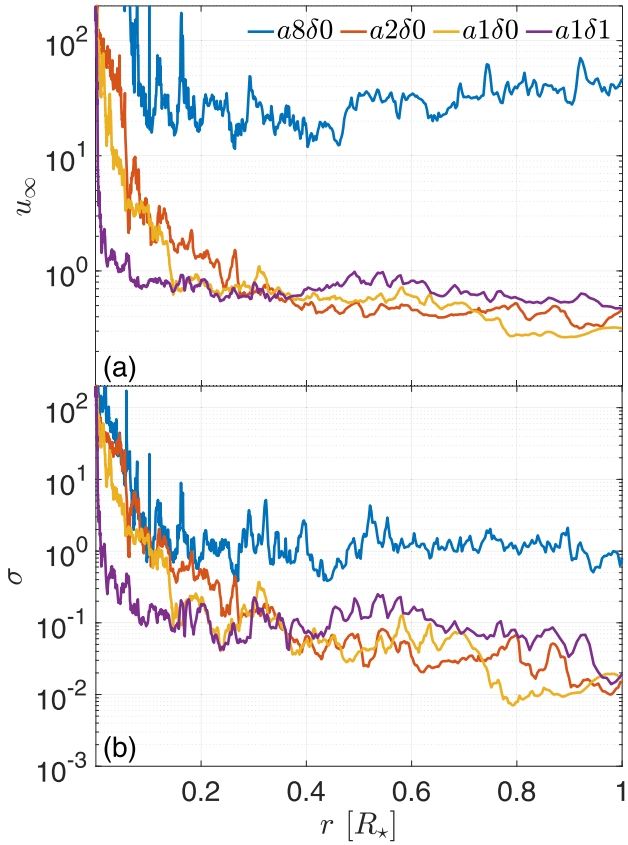

Figure 3. Radial profiles of the asymptotic proper velocity (a) and magnetization (b) of the jets inside the star, calculated by the maximum value at each radius at time t_s. The powerful jet (model $a8\delta0$) maintains relativistic velocities and mild magnetization, whereas the weaker jets undergo strong mixing with the star so they exhibit a mildly relativistic breakout with a low magnetization.

features a moderate level of magnetization. Both weaker jets dissipate most of their magnetic energy by mixing with the star, and break out with a negligible degree of magnetization while losing their collimated structure.

Figure 3 depicts the radial profiles of the "jet" asymptotic proper velocity u_∞ (panel (a)) and magnetization σ (panel (b)), defined as

$$u_\infty \equiv \sqrt{u_t^2\left(1+\frac{4p}{\rho c^2}+\sigma\right)^2-1}\,, \tag{9}$$

where ρ is the comoving mass density, p is the comoving gas pressure, u_t is the covariant time component of the four-velocity, $\sigma=\frac{B^2}{8\pi\rho c^2}$ is the magnetization, and B is the comoving magnetic field. The powerful jet launched by the rapidly spinning BH retains a moderate magnetization level and reaches the ultrarelativistic velocities of GRBs (blue lines). Conversely, the jets powered by the slowly spinning BHs lose most of their magnetic energy deep inside the stellar core due to mixing. As a result, they lose their ability to convert that energy to kinetic form and reach relativistic velocities. We emphasize that although mixing reduces the jets' velocities, their power upon breakout remains similar to their power upon launching. This raises the question of how such jets can reach asymptotic relativistic velocities to match both the GRB power and velocity. This problem might be alleviated if the jets were to be launched with $\sigma_0 \gg 10^3$, similar to the trend observed between the different σ_0 values in Gottlieb et al. (2022b). Unfortunately, present-day numerical codes cannot handle jet evolution at such high σ values.

4. Discussion

In this letter we show that theoretical considerations combined with GRB observations support the idea that collapsar BHs are probably born slowly spinning. The reasoning relies on several straightforward arguments. The first is that the magnetic flux is saturated in an MAD state (if its value is below saturation, the jet fails to launch). Hence, the magnetic-driven jet power depends only on the mass accretion rate and jet launching efficiency. Halevi et al. (2023) recently showed that at the time of BH formation, the inner stellar envelope has a universal radial density profile with a power-law index of -1.5. This is translated to a roughly constant mass accretion rate that, for a typical progenitor star with a few tens of solar mass, is $\dot{m} \simeq 10^{-2}\,M_\odot\ \mathrm{s}^{-1}$. Numerical models also feature constant jet launching efficiencies, so a constant accretion rate also implies no time evolution in the GRB light curve, as suggested by observations. This leaves the jet power to depend solely on the value of the jet launching efficiency, which in turn depends only on the BH spin. GRB prompt emission observations thus provide a direct connection between observables and BH spin.

We show that wobbling jets, as found in our simulations, require a dimensionless spin of $a \approx 0.5$ in order to match observed luminosities. If the jet is roughly axisymmetric, as traditional jet structure models suggest, a milder $a \approx 0.2$ is needed to launch a jet that produces the observed GRB luminosities. The above moderate spins correspond to low jet launching efficiency, implying that most of the accreted energy onto the BH is used for its mass growth rather than launching jets. In addition to the jet motion and opening angle, there are another two important caveats to this result: (i) the uncertainty in the jet radiative efficiency—if $\epsilon_\gamma \ll 1$, then the inferred BH spin would be significantly larger; and (ii) in our analysis of inferring the BH spin for axisymmetric jets, we assume that the entire jet is observed, thus ignoring cases in which the jet is observed slightly off-axis such that only part of its energy reaches the observer (e.g., Ito et al. 2019). If most GRBs are observed off-axis, then the jet energy, and the BH spin, could be significantly higher. Regardless of the value of the inferred spin, this value might hold true for the entire core-collapse BH population, unless there is an anticorrelation between the magnetic field strength in the star and the angular momentum of the star (e.g., through the magnetic Tayler instability), in which case BHs without jets spin faster. Namely, GRB observations indicate that the natal spin of the majority of newly formed BHs is small, otherwise there will be an excess of very powerful GRB jets in the Universe.

We verify our results by carrying out first-principles collapsar simulations, and show for the first time that slowly spinning BHs can launch relativistic jets with a typical GRB power, thereby supporting the above theoretical arguments. We find that the jet power does not change over time, but less powerful jets undergo intense mixing, even when a lower-density region along the poles is present. Consequently, the jets escape from the star being mildly relativistic and cannot reproduce the GRB observables. A possible solution to this

problem is an initial jet magnetization of $\sigma_0 \gg 10^3$, which may enable the jets to remain relativistic even after dissipating a substantial fraction of their magnetic energy.

While a moderate BH spin of $a \simeq 0.2$ can generate typical GRB jets of power $L_j \approx 10^{50}\,\mathrm{erg\,s^{-1}}$, the GRB energy distribution spans a vast range of many orders of magnitude. At the low end of the GRB luminosity distribution lie jets with $L_j \lesssim 10^{48}\,\mathrm{erg\,s^{-1}}$ (Wanderman & Piran 2010; Shahmoradi & Nemiroff 2015), which begs the question of what factors would support their emergence. Regardless of how such jets find their way out of the collapsing star, the fixed jet power throughout its propagation and Equation (3) dictate that these jets must be launched from a BH with a spin of $a \simeq 0.02$. However, for such a spin, the disk winds may outshine the jet and disrupt its emergence. Furthermore, in Jacquemin-Ide et al. (2023) we show that BHs with an initial spin of $a \lesssim 0.1$ inevitably spin up to $a \simeq 0.1$ before the jet breaks out. Therefore, low-power jets likely emerge from a BH with $a \approx 0.1$, but with a lower accretion rate.

At the high end of the GRB energy distribution, powerful jets require a BH spin close to unity. However, in Jacquemin-Ide et al. (2023) we show that the BH likely spins up to high spins rather than having a high natal spin. This implies that conceivably all collapsar BHs are born slowly spinning, and when the magnetic field profile of the star is such that the development of the MAD state is delayed, the BH may spin up to $a \approx 0.5$ before the MAD state fully develops. Once the system is MAD, the BH will spin down and reach a low final spin, $a \approx 0.1$. Thus, the high spin is only achieved for a relatively short time.

As most collapsar BHs have $a \lesssim 0.2$, our simulations indicate that they would produce jets that struggle to break out relativistically from stars, and it is likely that some of those jets would fail to generate the GRB emission. Instead, the jets will energize the expansion of the shocked jet material that will ultimately break out and radiate a softer emission that could be associated with sub- and mildly relativistic transients. This conclusion is obtained for the first time from a computational perspective, supporting the idea that many collapsar jets are choked based on the GRB duration distribution (Bromberg et al. 2012).

Here we study the effect of the initial BH spin on jet launching, assuming a BH spin that does not change in time. In reality, the BH spins up by accreting angular momentum from the infalling gas, and spins down by utilizing its rotational energy to launch the jets. These effects are particularly important when the BH spin is far from the equilibrium spin of $a \approx 0.1$ (Lowell et al. 2023). In a companion paper (Jacquemin-Ide et al. 2023), we show that taking into account the BH spin evolution does not change our conclusion that disfavors rapidly spinning BHs. The reason is that the mass accretion rate is not high enough to introduce a significant spin-down within the jet breakout time from the star. Furthermore, in Jacquemin-Ide et al. (2023) we show that even if the BH were to be initially rapidly spinning, for any reasonable set of physical parameters, it eventually spins down close to the equilibrium spin.

Acknowledgments

We thank the referee for helpful comments. O.G. is supported by a CIERA Postdoctoral Fellowship. O.G. and A. T. acknowledge support by Fermi Cycle 14 Guest Investigator program 80NSSC22K0031. J.J. and A.T. acknowledge support by the NSF AST-2009884 and NASA 80NSSC21K1746 grants. B.L. acknowledges support by a National Science Foundation Graduate Research Fellowship under grant No. DGE-2234667. B.L. also acknowledges support by a Illinois Space Grant Consortium (ISGC) Graduate Fellowship supported by a National Aeronautics and Space Administration (NASA) grant awarded to the ISGC. A.T. was also supported by NSF grants AST-2107839, AST-1815304, AST-1911080, AST-2206471, and OAC-2031997, and NASA grant 80NSSC18K0565. Support for this work was also provided by the National Aeronautics and Space Administration through Chandra Award Number TM1-22005X issued by the Chandra X-ray Center, which is operated by the Smithsonian Astrophysical Observatory for and on behalf of the National Aeronautics Space Administration under contract NAS8-03060. This research used resources of the Oak Ridge Leadership Computing Facility, which is a DOE Office of Science User Facility supported under Contract DE-AC05-00OR22725. An award of computer time was provided by the ASCR Leadership Computing Challenge (ALCC), Innovative and Novel Computational Impact on Theory and Experiment (INCITE), and OLCF Director's Discretionary Allocation programs under award PHY129. This research used resources of the National Energy Research Scientific Computing Center, a DOE Office of Science User Facility supported by the Office of Science of the U.S. Department of Energy under Contract No. DE-AC02-05CH11231 using NERSC award ALCC-ERCAP0022634.

Data Availability

The data underlying this article will be shared upon reasonable request to the corresponding author.

ORCID iDs

Ore Gottlieb https://orcid.org/0000-0003-3115-2456
Jonatan Jacquemin-Ide https://orcid.org/0000-0003-2982-0005
Beverly Lowell https://orcid.org/0000-0002-2875-4934
Alexander Tchekhovskoy https://orcid.org/0000-0002-9182-2047
Enrico Ramirez-Ruiz https://orcid.org/0000-0003-2558-3102

References

Abbott, R., Abbott, T. D., Abraham, S., et al. 2020, ApJL, 896, L44
Aloy, M. Á., & Obergaulinger, M. 2021, MNRAS, 500, 4365
Bavera, S. S., Fragos, T., Zapartas, E., et al. 2022, A&A, 657, L8
Belczynski, K., Klencki, J., Fields, C. E., et al. 2020, A&A, 636, A104
Belczynski, K., Wiktorowicz, G., Fryer, C. L., Holz, D. E., & Kalogera, V. 2012, ApJ, 757, 91
Blandford, R. D., & Znajek, R. L. 1977, MNRAS, 179, 433
Bromberg, O., Nakar, E., Piran, T., & Sari, R. 2012, ApJ, 749, 110
Bromberg, O., & Tchekhovskoy, A. 2016, MNRAS, 456, 1739
Burrows, A., Dessart, L., Livne, E., Ott, C. D., & Murphy, J. 2007, ApJ, 664, 416
Cantiello, M., Yoon, S. C., Langer, N., & Livio, M. 2007, A&A, 465, L29
De Donder, E., & Vanbeveren, D. 1998, A&A, 333, 557
de Mink, S. E., Langer, N., Izzard, R. G., Sana, H., & de Koter, A. 2013, ApJ, 764, 166
Duchêne, G., & Kraus, A. 2013, ARA&A, 51, 269
Eichler, D., Livio, M., Piran, T., & Schramm, D. N. 1989, Natur, 340, 126
Eichler, D., & Waxman, E. 2005, ApJ, 627, 861
Farr, W. M., Sravan, N., Cantrell, A., et al. 2011, ApJ, 741, 103

Farr, W. M., Stevenson, S., Miller, M. C., et al. 2017, Natur, 548, 426
Frail, D. A., Kulkarni, S. R., Sari, R., et al. 2001, ApJL, 562, L55
Fryer, C. L., & Heger, A. 2005, ApJ, 623, 302
Fryer, C. L., Mazzali, P. A., Prochaska, J., et al. 2007, PASP, 119, 1211
Fujibayashi, S., Sekiguchi, Y., Shibata, M., & Wanajo, S. 2022, arXiv:2212.03958
Fujibayashi, S., Shibata, M., Wanajo, S., et al. 2020, PhRvD, 102, 123014
Fuller, J., & Ma, L. 2019, ApJL, 881, L1
Goldstein, A., Connaughton, V., Briggs, M. S., & Burns, E. 2016, ApJ, 818, 18
Gottlieb, O., Bromberg, O., Levinson, A., & Nakar, E. 2021a, MNRAS, 504, 3947
Gottlieb, O., Nakar, E., & Bromberg, O. 2021b, MNRAS, 500, 3511
Gottlieb, O., Bromberg, O., Singh, C. B., & Nakar, E. 2020a, MNRAS, 498, 3320
Gottlieb, O., Levinson, A., & Nakar, E. 2020b, MNRAS, 495, 570
Gottlieb, O., Lalakos, A., Bromberg, O., Liska, M., & Tchekhovskoy, A. 2022a, MNRAS, 510, 4962
Gottlieb, O., Liska, M., Tchekhovskoy, A., et al. 2022b, ApJL, 933, L9
Gottlieb, O., Nagakura, H., Tchekhovskoy, A., et al. 2023, ApJL, 951, L30
Gottlieb, O., Tchekhovskoy, A., & Margutti, R. 2022d, MNRAS, 513, 3810
Gottlieb, O., Levinson, A., & Nakar, E. 2019, MNRAS, 488, 1416
Halevi, G., Wu, B., Mösta, P., et al. 2023, ApJL, 944, L38
Harrison, R., Gottlieb, O., & Nakar, E. 2018, MNRAS, 477, 2128
Hoy, C., Fairhurst, S., Hannam, M., & Tiwari, V. 2022, ApJ, 928, 75
Ito, H., Matsumoto, J., Nagataki, S., et al. 2019, NatCo, 10, 1504
Ito, H., Matsumoto, J., Nagataki, S., Warren, D. C., & Barkov, M. V. 2015, ApJL, 814, L29
Izzard, R. G., Ramirez-Ruiz, E., & Tout, C. A. 2004, MNRAS, 348, 1215
Jacquemin-Ide, J., Gottlieb, O., Lowell, B., & Tchekhovskoy, A. 2023, arXiv:2302.07281
Janiuk, A., & Yuan, Y. F. 2010, A&A, 509, A55
Kawanaka, N., Piran, T., & Krolik, J. H. 2013, ApJ, 766, 31
Kobulnicky, H. A., & Fryer, C. L. 2007, ApJ, 670, 747
Kochanek, C. S. 2015, MNRAS, 446, 1213
Komissarov, S. S., & Barkov, M. V. 2009, MNRAS, 397, 1153
Lee, W. H., & Ramirez-Ruiz, E. 2006, ApJ, 641, 961
Liska, M. T. P., Chatterjee, K., Issa, D., et al. 2022, ApJS, 263, 26
López-Cámara, D., Lazzati, D., & Morsony, B. J. 2016, ApJ, 826, 180
López-Cámara, D., Morsony, B. J., Begelman, M. C., & Lazzati, D. 2013, ApJ, 767, 19
Lowell, B., Jacquemin-Ide, J., Tchekhovskoy, A., & Duncan, A. 2023, arXiv:2302.01351
Lyutikov, M., & Blandford, R. 2003,
MacFadyen, A. I., & Woosley, S. E. 1999, ApJ, 524, 262
Margalit, B., & Metzger, B. D. 2017, ApJL, 850, L19
McBreen, S., McBreen, B., Hanlon, L., & Quilligan, F. 2002, A&A, 393, L29
Middleton, M. 2016, Astrophysics of Black Holes, Astrophysics and Space Science Library, Vol. 440 (Berlin: Springer), 99
Obergaulinger, M., & Aloy, M. Á. 2022, MNRAS, 512, 2489
Offner, S. S. R., Clark, P. C., Hennebelle, P., et al. 2014, in Protostars and Planets VI, ed. H. Beuther et al. (Tucson, AZ: Univ. of Arizona Press), 53
Özel, F., Psaltis, D., Narayan, R., & McClintock, J. E. 2010, ApJ, 725, 1918
Panaitescu, A., & Kumar, P. 2002, ApJ, 571, 779
Penrose, R., & Floyd, R. M. 1971, NPhS, 229, 177
Petrovic, J., Langer, N., Yoon, S. C., & Heger, A. 2005, A&A, 435, 247
Popham, R., Woosley, S. E., & Fryer, C. 1999, ApJ, 518, 356
Reynolds, C. S. 2021, ARA&A, 59, 117
Roulet, J., & Zaldarriaga, M. 2019, MNRAS, 484, 4216
Safarzadeh, M., Farr, W. M., & Ramirez-Ruiz, E. 2020, ApJ, 894, 129
Sana, H., de Mink, S. E., de Koter, A., et al. 2012, Sci, 337, 444
Shahmoradi, A., & Nemiroff, R. J. 2015, MNRAS, 451, 126
Smith, N., Li, W., Filippenko, A. V., & Chornock, R. 2011, MNRAS, 412, 1522
Tchekhovskoy, A. 2015, in The Formation and Disruption of Black Hole Jets, Astrophysics and Space Science Library, ed. I. Contopoulos, D. Gabuzda, & N. Kylafis, Vol. 414 (Berlin: Springer), 45
Tchekhovskoy, A., & Giannios, D. 2015, MNRAS, 447, 327
Tchekhovskoy, A., Narayan, R., & McKinney, J. C. 2011, MNRAS, 418, L79
Tiwari, V., Fairhurst, S., & Hannam, M. 2018, ApJ, 868, 140
Wanderman, D., & Piran, T. 2010, MNRAS, 406, 1944
Woosley, S. E., & Heger, A. 2006, ApJ, 637, 914
Yoon, S. C., Woosley, S. E., & Langer, N. 2010, ApJ, 725, 940